Energy-Aware Resilience: An Energy-State-Driven Restoration for Hydrogen-Integrated Power Systems

Airin Rahman, Md Moshiur Rahman, and Wei Sun
Department of Electrical and Computer Engineering, University of Central Florida, Orlando, Florida, USA
Emails: airin.rahman@ucf.edu, md.moshiur.rahman@ucf.edu, sun@ucf.edu

***Abstract*—Frequent extreme events and large-scale blackouts highlight the need for adaptive, energy-aware restoration in renewable-dominated power systems. Conventional methods follow fixed energization sequences that overlook the real-time availability of stored energy, often causing inefficient recovery or premature resource depletion. This paper presents an energy-state-driven adaptive restoration (ESDAR) framework for hydrogen-integrated, resilience-oriented recovery of power systems. ESDAR directly links restoration scheduling to the hydrogen energy state of distributed long-duration energy storage (LDES) units and dynamically adjusts the number of network elements energized at each stage according to the remaining reserves, allowing the restoration pace to self-regulate as stored energy declines. A lightweight switching and scheduling formulation captures line activation limits and operational constraints with computational efficiency, while a resilience phase-space visualization depicts the co-evolution of hydrogen energy, restored load, and network activation. Simulation studies on a modified IEEE 39-bus system show that ESDAR restores 12%–15% more cumulative load and achieves an 11% higher resilience index than fixed strategies. The results demonstrate that the proposed framework enhances operational stability and offers a practical pathway to self-regulating resilience in renewable-rich and islanded power grids.**

***Index Terms*—Adaptive restoration, dynamic scheduling, energy-state-driven control, grid resilience, hydrogen energy systems, long-duration energy storage.**

I. Introduction

Modern power systems are undergoing rapid transformation under the twin imperatives of *decarbonization* and *decentralization*. As renewable generation and long-duration energy storage (LDES) technologies proliferate, the grid becomes cleaner yet increasingly complex, particularly under extreme events such as hurricanes, wildfires, and cyber-physical threats or disruptions [1]. These disturbances test not only the grid's ability to survive but also its capacity to *recover adaptively*. Achieving true grid resilience therefore demands restoration strategies that dynamically respond to evolving energy states rather than relying on static methods designed for a more predictable grid environment.

Traditionally, post-blackout restoration follows fixed, rule-based sequences: transmission first, then sub-transmission, and finally distribution feeders according to predefined priorities. While this ensures safety and coordination, it remains fundamentally *energy-blind*. In renewable-rich systems, restoration success depends critically on the available stored energy at each recovery step [2], [3]. Once local storage is depleted, even meticulously planned sequences may stall, leading to incomplete or delayed system recovery.

Hydrogen-based LDES has emerged as a cornerstone of grid resilience strategies, bridging intermittent renewables and demand through reversible power-to-hydrogen and hydrogen-to-power processes [4]. Recent studies highlight hydrogen's role in enhancing resilience and coordinated restoration [5]–[7], while broader analyses of LDES emphasize their economic and system-level potential [8], [9]. However, most of these efforts focus on capacity planning, market integration, or long-term system optimization, leaving the development of real-time, energy-governed restoration strategies capable of adapting dynamically to depleting storage largely unexplored.

Meanwhile, progress in intelligent restoration has produced expert systems, adaptive decision-making strategies, and restoration decision-support systems [10]–[12]. Advanced frameworks such as hierarchical modern power system restoration with GNN and distributionally robust optimization [13] or LSTM-based adaptive algorithms for load prioritization [14] have enhanced flexibility and situational awareness. Yet, these methods rely on predefined restoration hierarchies that are decoupled from real-time energy-state feedback, limiting their ability to self-regulate restoration pace, optimize energy utilization, and sustain recovery under extreme conditions.

To bridge this gap, this paper introduces an **energy-state-driven adaptive restoration (ESDAR)** framework for hydrogen-integrated, resilience-oriented post-blackout recovery of the grid under extreme events. Unlike conventional tiered approaches, ESDAR establishes an adaptive restoration hierarchy in which the number of buses, feeders, or lines energized at each stage is governed by the *real-time energy-state* within distributed LDES units. As reserves decline, the restoration pace self-adjusts, maintaining a balanced, energy-aware, and self-regulating recovery process that remains robust under compound disruptions. In essence, ESDAR reframes hydrogen not as a passive energy reserve but as an active governor of system resilience, linking stored energy directly to restoration pace and decision-making.

The framework combines a lightweight switching and scheduling formulation, which respects operational limits and line activation constraints with a novel resilience phase-space visualization that illustrates the co-evolution of hydrogen energy, restored load, and network activation. Together, these elements transform restoration from a static, rule-based procedure into a dynamic, energy-informed process that adapts autonomously to changing system conditions. This energy-state-driven paradigm represents a step toward self-organizing

979-8-3315-8138-1

recovery, offering a practical and computationally efficient pathway to enhance resilience in renewable-dominated and islanded power systems. The key contributions of this paper are summarized as follows:

- Proposes a framework which establishes a linear, energy-dependent constraint that dynamically links hydrogen availability to network energization, enabling adaptive restoration depending on remaining storage resources.
- Reinterprets hydrogen-based LDES as an active restoration enabler that governs restoration speed, energization hierarchy, and the overall extent of system recovery.
- Incorporates realistic switching limits and introduces a resilience phase-space visualization to enhance operator awareness and decision support during restoration.

The remainder of the paper is organized as follows. Section II describes the proposed ESDAR framework and its mathematical formulation. Section III presents the simulation setup and discusses the results, while Section IV concludes the paper with key insights and future research directions.

II. Proposed Framework

A. Concept Overview

The proposed ESDAR framework establishes a dynamic operational link between the real-time energy availability in hydrogen-based LDES units and the pace of power system recovery during extreme events. Rather than following fixed hierarchical sequences, ESDAR enables a *living restoration hierarchy*, one that evolves according to the state of stored energy across the network.

During blackout or islanded operation, each hydrogen system operates in fuel-cell mode, supplying power to local loads or designated black-start nodes using its pre-stored hydrogen reserves. The aggregated hydrogen energy fraction,

$$\phi_t = \frac{\sum_h H_{h,t}^{st}}{\sum_h H_h^{st,\max}},$$

serves as a global indicator of available resilience resources at time step t. This variable is embedded directly within the restoration optimization, constraining the incremental activation of downstream network elements as

$$\sum_{n\in\mathcal{N}} \left(x_{n,t}^{\text{bus}} - x_{n,t-1}^{\text{bus}}\right) \le \kappa_0 + \kappa_1 \phi_t,$$

where κ_0 and κ_1 represent the baseline and energy-proportional restoration capacities, respectively. As hydrogen reserves are consumed, the value of ϕ_t declines, automatically reducing the allowable rate of new bus or feeder activations. In effect, the grid *self-regulates* its restoration pace in proportion to its remaining energy, ensuring that recovery remains both operationally safe and energy-aware.

This adaptive formulation transforms hydrogen energy from a passive backup reserve into an active control signal that governs the tempo of restoration. Without relying on predefined switching orders, ESDAR continuously synchronizes restoration actions with real-time energy conditions, providing operators with a natural feedback loop between *available energy* and *restoration progress*.

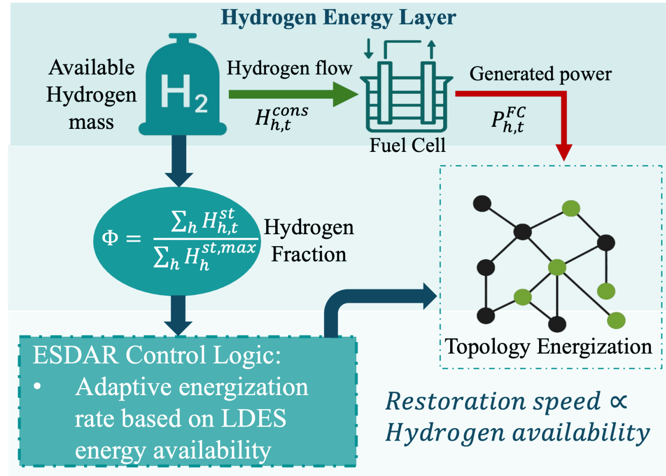

Fig. 1. ESDAR Framework: Linking hydrogen energy availability with adaptive network energization.

The framework can be seamlessly integrated with lightweight line-switching and power-flow formulations, enabling fast computation and intuitive interpretation. In doing so, it offers a practical, operator-oriented scheduling tool for post-blackout decision support, bridging physical energy states with actionable restoration strategies.

Fig. 1 illustrates the conceptual framework of the proposed ESDAR, where real-time hydrogen availability governs adaptive control logic that dynamically adjusts network energization to achieve balanced, energy-aware system recovery.

B. Mathematical Formulation

The proposed ESDAR model is formulated as a mixed-integer linear program (MILP) that co-optimizes hydrogen fuel-cell power dispatch and network restoration scheduling under energy-availability constraints. The formulation integrates four interacting components: (i) power balance, (ii) hydrogen discharge and storage dynamics, (iii) switching and energization logic, and (iv) the energy-state-driven hierarchy.

1) Objective Function: The optimization maximizes the total served load while penalizing excessive switching effort:

$$\max \sum_{t\in\mathcal{T}} \sum_{n\in\mathcal{N}} \ell_{n,t} - \lambda \sum_{t\in\mathcal{T}} \sum_{\ell\in\mathcal{L}} u_{\ell,t}^{\text{line}}, \tag{1}$$

where $\ell_{n,t}$ represents the active load served at bus n and time t, and λ is a weighting coefficient balancing restoration benefit and operational effort.

2) Initialization and Monotonicity: At the initial time step, seed buses $\mathcal{E}$ (e.g., hydrogen–fuel-cell sites) are energized. Once energized, buses remain active for the remainder of the restoration horizon:

$$x_{n,1}^{\text{bus}} = 1,\ \forall n \in \mathcal{E}, \qquad x_{n,t}^{\text{bus}} \ge x_{n,t-1}^{\text{bus}},\ \forall n,\ t > 1. \tag{2}$$

3) Line Gating and Switching Constraints: A line can be active only if both terminal buses are energized:

$$x_{(i,j),t}^{\text{line}} \le x_{i,t}^{\text{bus}}, \quad x_{(i,j),t}^{\text{line}} \le x_{j,t}^{\text{bus}},\ \forall (i,j), t. \tag{3}$$

979-8-3315-8138-1

Switching actions are captured by auxiliary binary variables $u_{\ell,t}^{\text{line}}$:

$$u_{(i,j),t}^{\text{line}} \geq x_{(i,j),t}^{\text{line}} - x_{(i,j),t-1}^{\text{line}}, \quad t > 1, \tag{4}$$

$$\sum_{\ell \in \mathcal{L}} u_{\ell,t}^{\text{line}} \leq \bar{U}_t, \quad \forall t, \tag{5}$$

$$x_{\ell,t}^{\text{line}} \geq x_{\ell,t-1}^{\text{line}}, \quad \forall \ell, t > 1. \tag{6}$$

Constraint (5) limits the number of allowed switching operations per time step to emulate practical field constraints. This formulation prevents non-physical re-opening of previously energized lines and ensures a monotonically expanding restoration frontier. By using a small per-step switching budget $\bar{U}_t$, the model remains computationally tractable while reflecting the finite operational capacity of field crews or automated breakers during restoration.

4) Power Flow and Balance: To ensure network feasibility during the restoration process, power exchange among connected buses is modeled based on relative voltage angles and limited by the thermal capacities of the energized lines. At each bus n and time step t:

$$\theta_{n_0,t} = 0, \quad \forall t, \tag{7}$$

$$f_{(i,j),t} = B_{(i,j)}(\theta_{i,t} - \theta_{j,t}), \ \forall (i,j), t, \tag{8}$$

$$-\bar{F}_{(i,j)} x_{(i,j),t}^{\text{line}} \leq f_{(i,j),t} \leq \bar{F}_{(i,j)} x_{(i,j),t}^{\text{line}}, \ \forall (i,j), t, \tag{9}$$

$$\sum_{(n,j)} f_{(n,j),t} - \sum_{(i,n)} f_{(i,n),t} = P_{n,t}^{\text{FC}} - \ell_{n,t}, \ \forall n, t, \tag{10}$$

$$0 \leq \ell_{n,t} \leq d_{n,t}\, x_{n,t}^{\text{bus}}, \quad 0 \leq P_{h,t}^{\text{FC}} \leq \bar{P}_h^{\text{FC}}\, x_{h,t}^{\text{bus}}, \quad \ell_{n,t} \geq 0. \tag{11}$$

Equation (8) models power transfer between connected buses based on voltage angle differences, while (9) enforces line transfer limits. The nodal balance (10) maintains equality between fuel-cell generation, load demand, and network exchanges at each time step.

5) Fuel Cell Discharge Dynamics: During blackout operation, each hydrogen-based LDES unit operates solely in fuel-cell (FC) discharge mode to supply electricity to local loads or downstream buses. The process is modeled as a continuous relationship between hydrogen consumption and electrical power output, without binary operational states:

$$0 \leq H_{h,t}^{\text{cons}} \leq \bar{H}_h^{\text{cons}}\, x_{h,t}^{\text{bus}}, \qquad \forall h, t, \tag{12}$$

$$P_h^{\text{FC,min}}\, x_{h,t}^{\text{bus}} \leq P_{h,t}^{\text{FC}} \leq P_h^{\text{FC,max}}\, x_{h,t}^{\text{bus}}, \qquad \forall h, t, \tag{13}$$

$$P_{h,t}^{\text{FC}} = \alpha_h^{\text{FC}}\, H_{h,t}^{\text{cons}}, \qquad \forall h, t. \tag{14}$$

where, $H_{h,t}^{\text{cons}}$ [kg/h] denotes the hydrogen consumption rate, $P_{h,t}^{\text{FC}}$ [MW] is the generated power, and $\alpha_h^{\text{FC}} = \gamma_h^{\text{FC}} \eta_h^{\text{FC}}$ represents the combined hydrogen-to-electric conversion factor (MW per kg/h) [15]. Equations (12)–(14) ensure that the fuel-cell output remains within stack limits while preserving model linearity and computational efficiency for each simulation interval.

6) Hydrogen Storage Intertemporal Dynamics: Hydrogen tank storage evolves according to the mass balance between consecutive time steps:

$$H_{h,t}^{st} = H_{h,t-1}^{st} - H_{h,t}^{\text{cons}}\, \Delta t, \quad \forall h, t > 1, \tag{15}$$

with initialization

$$H_{h,1}^{st} = H_h^{st,\text{init}}, \tag{16}$$

and operational limits

$$H_h^{st,\text{min}} \leq H_{h,t}^{st} \leq H_h^{st,\text{max}}, \quad H_{h,t}^{st} \geq 0, \quad \forall h, t. \tag{17}$$

Equation (15) enforces intertemporal coupling of stored hydrogen, while (17) preserves safety margins on tank pressure and reserves.

7) Energy-State-Driven Hierarchy: The aggregated hydrogen energy fraction ϕ_t represents the normalized, system-wide energy availability and directly regulates restoration pacing:

$$\phi_t = \frac{\sum_{h \in \mathcal{H}} H_{h,t}^{st}}{H^{st,\text{den}}}, \quad H^{st,\text{den}} = \sum_{h \in \mathcal{H}} H_h^{st,\text{max}} > 0. \tag{18}$$

The rate of new bus energization is adaptively limited by this fraction:

$$\sum_{n \in \mathcal{N}} \left(x_{n,t}^{\text{bus}} - x_{n,t-1}^{\text{bus}} \right) \leq \kappa_0 + \kappa_1\, \phi_t, \quad t > 1, \tag{19}$$

where κ_0 and κ_1 are tuning coefficients that define the baseline and energy-proportional restoration capacities. As ϕ_t decreases due to hydrogen depletion, the model automatically slows the restoration rate, providing a self-regulating, energy-aware mechanism that links physical storage conditions to restoration scheduling.

III. Simulation and Results analysis

A. Simulation Setup

The proposed ESDAR framework is evaluated on the IEEE 39-bus test system, which is modified to emulate an islanded operating condition under a complete grid blackout. Hydrogen-based LDES units are deployed at buses 16, 21, 33, and 36 to enable distributed black-start and local restoration capability. Each LDES unit comprises a fuel cell and a hydrogen storage tank operating exclusively in discharge mode during the restoration period. No grid import or photovoltaic generation is assumed; thus, the stored hydrogen energy represents the sole source of supply throughout the restoration process.

The simulation horizon spans 12 hours with a 10-minute time resolution ($\Delta t = 10/60$ h), yielding 72 scheduling intervals. The initial hydrogen energy states are varied to represent different resilience conditions as

$$E_{h,1}/E_h^{\max} \in \{0.35,\, 0.50,\, 0.70\},$$

corresponding to low, medium, and high hydrogen available levels. The per-interval switching budget is constrained to $\bar{U}_t = 1$ line activations, while the coefficients of the energy-state-driven constraint are set to $\kappa_0 = 1$ and $\kappa_1 = 6$, calibrated to ensure gradual and energy-aware restoration progression.

B. Results and Discussion

The performance of the proposed ESDAR framework is evaluated under islanded operation, where hydrogen-based LDES units act as the sole energy source. The results are compared against a conventional fixed-sequence restoration approach, which energizes network elements in a predetermined order without accounting for real-time energy availability.

979-8-3315-8138-1

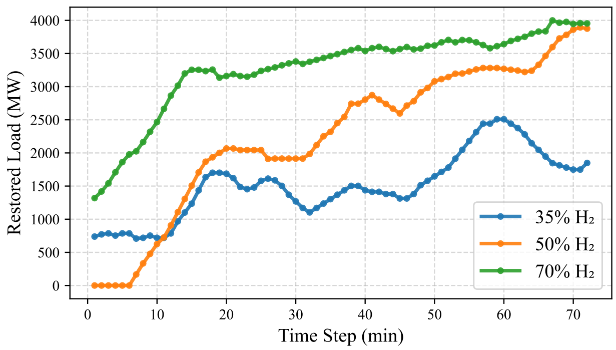

Fig. 2. Restored load trajectories under varying initial hydrogen availability.

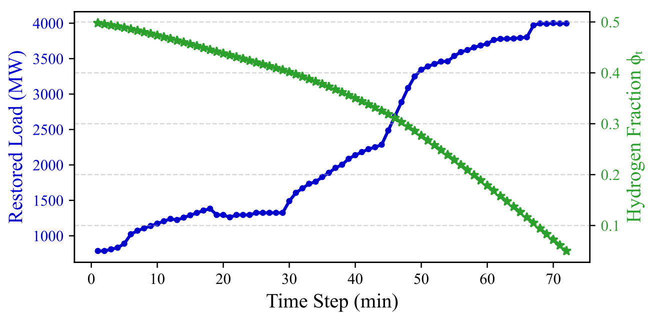

Fig. 3. Dynamic coupling between hydrogen energy fraction and restored load.

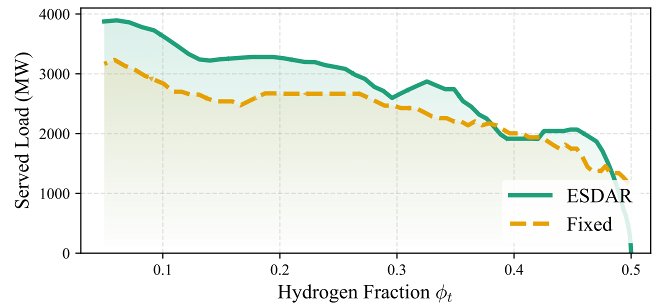

Fig. 4. Resilience phase-space trajectory between hydrogen energy and served load.

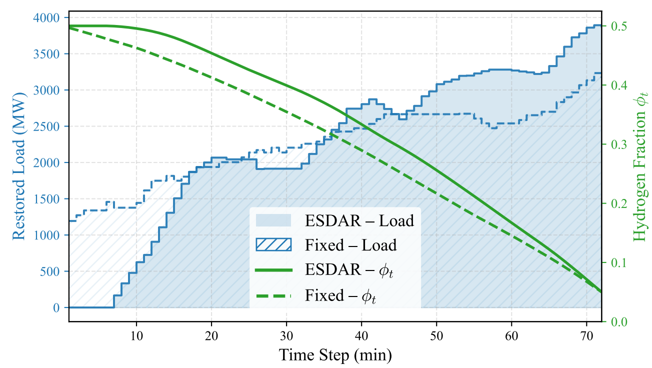

Fig. 5. Comparison of restored load trajectories under ESDAR and fixed restoration logic.

1) Restoration Behavior under Varying Hydrogen Availability: Fig. 2 presents the restored load trajectories for different initial hydrogen mass. When the available hydrogen reserve increases from 35% to 70%, the restoration process becomes significantly faster, resulting in higher cumulative load recovery within the same time horizon. At low hydrogen availability (35%), restoration progress is slow and intermittent due to limited available energy, while higher amount of hydrogen levels support continuous network energization and smoother load pickup. This behavior confirms the adaptive property of ESDAR, where the restoration pace naturally scales with the available hydrogen energy, ensuring an energy-aware and stable recovery process.

2) Hydrogen–Load Interaction and Dynamic Coupling: Fig. 3 shows the temporal evolution of restored load and hydrogen energy fraction. As hydrogen is consumed, the available fraction ϕ_t steadily declines while the restored load rises in a coordinated manner. The adaptive restoration initially proceeds at a moderate pace, accelerates with sufficient hydrogen availability, and gradually slows as reserves diminish. This co-evolution demonstrates the self-regulating behavior of the proposed framework, restoration speed adapts automatically to available hydrogen energy, ensuring efficient utilization of stored resources and preventing premature depletion. As a result, the system follows a smooth, balanced recovery trajectory in which hydrogen availability directly governs restoration progress and load recovery.

3) Resilience Phase-Space Representation: The coupled evolution of hydrogen depletion and load restoration is illustrated in the resilience phase-space of Fig. 4. The ESDAR trajectory forms a smooth, monotonic curve, indicating stable and efficient conversion of hydrogen energy into delivered power. As hydrogen reserves decline, the adaptive restoration logic moderates energization speed, sustaining higher load service for longer durations. In contrast, the fixed-sequence approach shows irregular fluctuations and a consistently lower served load for the same hydrogen availability, reflecting inefficient energy use and the absence of dynamic feedback. The elevated and continuous ESDAR trajectory confirms that the proposed energy-aware logic effectively translates stored hydrogen into sustained recovery, enhancing both energy-to-load efficiency and system resilience.

Although omitted here for brevity, the corresponding energy-to-load efficiency analysis exhibits the same pattern, ESDAR maintains higher conversion efficiency throughout the restoration period, whereas the fixed strategy suffers from early hydrogen depletion and declining performance. This further validates that adaptive, hydrogen-informed restoration enables more effective utilization of long-duration storage resources.

4) Comparative Restoration Performance: Fig. 5 compares the restoration trajectories of the ESDAR and fixed strategies. Under the adaptive ESDAR framework, restoration progresses

979-8-3315-8138-1

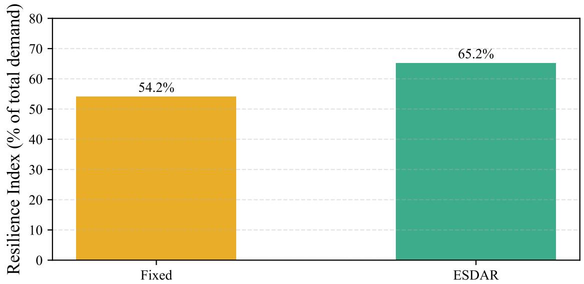

Fig. 6. Resilience index comparison between ESDAR and fixed restoration strategies.

smoothly, with a steady rise in served load and a controlled, gradual decline in hydrogen availability, indicating balanced and efficient energy use. In contrast, the fixed strategy exhibits a rapid initial load recovery followed by stagnation as hydrogen reserves are exhausted prematurely. This imbalance causes an abrupt energy drop and limits total load restoration. The comparison underscores ESDAR's ability to align restoration speed with available hydrogen, achieving greater cumulative load service, slower fuel depletion, and enhanced overall resilience.

5) Resilience Index Quantification: Fig. 6 compares the resilience performance of the two restoration strategies using the Resilience Index (RI), the ratio of total served energy to total demand over the restoration horizon. The proposed ESDAR framework achieves an RI of 65.2%, exceeding the fixed restoration strategy's 54.2%. This 11% improvement highlights how the energy-aware logic of ESDAR enables faster and more sustained recovery by dynamically aligning restoration decisions with available hydrogen energy. Incorporating real-time hydrogen feedback into the restoration process substantially enhances system resilience, supporting quicker, longer, and more reliable load restoration under islanded conditions.

Collectively, the results validate that the proposed ESDAR framework achieves an adaptive, energy-aware, and computationally efficient restoration process. By coupling restoration scheduling with the real-time hydrogen availability, ESDAR enhances total served load, prolongs supply duration, and improves energy utilization under constrained switching operations. The framework therefore provides a practical pathway toward resilient and self-regulating grid recovery in future renewable-dominated and islanded power systems.

IV. Conclusion

This paper introduced the ESDAR framework, which integrates hydrogen-based LDES into the power system restoration process. Unlike fixed restoration sequences, ESDAR dynamically links network energization with real-time hydrogen availability, allowing the restoration pace to self-adjust based on remaining energy. The proposed resilience phase-space visualization captures the co-evolution of hydrogen availability, restored load, and network activation, revealing smoother trajectories and higher energy-to-load efficiency.

Simulation results on the modified IEEE 39-bus system demonstrate that ESDAR restores 12%–15% more load and achieves an 11% higher RI than the fixed restoration approach while maintaining balanced hydrogen utilization. The formulation embeds practical switching limits and ramp constraints within a lightweight optimization structure, offering an efficient and decision support tool for energy-aware restoration. Future work will extend ESDAR into a robust, operator-in-the-loop framework by incorporating renewable and load uncertainties through distributed robust optimization and integrating human decision feedback. These advancements aim to deliver a more realistic, resilience-oriented restoration framework for future power grid.

References

[1] A. Rahman *et al.*, "Challenges and opportunities in cyber-physical security of highly der-penetrated power systems," in *2022 IEEE Power & Energy Society General Meeting (PESGM)*, 2022, pp. 1–5.

[2] Y. Liu, R. Fan, and V. Terzija, "Power system restoration: A literature review from 2006 to 2016," *Journal of Modern Power Systems and Clean Energy*, vol. 4, no. 3, pp. 332–341, 2016.

[3] G. Patsakis, D. Rajan, I. Aravena, J. Rios, and S. Oren, "Optimal black start allocation for power system restoration," *IEEE Transactions on Power Systems*, vol. 33, no. 6, pp. 6766–6776, 2018.

[4] J. Han, J. Wang, Z. He, Q. An, Y. Song, A. Mujeeb, C.-W. Tan, and F. Gao, "Hydrogen-powered smart grid resilience," *Energy Conversion and Economics*, vol. 4, no. 2, pp. 89–104, 2023.

[5] P. Xie, R. Zhao, Y. Chen, Y. Yang, Q. Yang, Y. Lin, and G. Li, "Resilience enhancement strategies for power distribution network based on hydrogen storage and hydrogen vehicle," *IET Energy Systems Integration*, vol. 6, no. S1, pp. 789–798, 2024.

[6] X. Chen, J. Liu, P. Li, J. Ren, D. Zhang, and X. Zhou, "A multi-stage resilience enhancement method for distribution networks employing transportation and hydrogen energy systems," *Sustainability*, vol. 17, no. 19, 2025.

[7] G. Hua, W. Li, and X. Huang, "New role of hydrogen systems in self-healing and service restoration of pv-dominated distribution network: Regret assessment methodology," *Renewable Energy*, vol. 254, p. 123409, 2025.

[8] A. Selänniemi, M. Hellström, and M. Björklund-Sänkiaho, "Long-duration energy storage—a literature review on the link between variable renewable energy penetration and market creation," *Energies*, vol. 17, no. 15, 2024.

[9] H. Ameli, D. Pudjianto, G. Strbac, and N. P. Brandon, "The impact of hydrogen on decarbonisation and resilience in integrated energy systems," *Advances in Applied Energy*, vol. 17, p. 100200, 2025.

[10] W. Ahmad, B. Shah, T. Hussain, S. EI-Sappagh, and F. Ali, "An expert system-based restoration method for energy services," *Sustainable Energy, Grids and Networks*, vol. 38, p. 101302, 2024.

[11] T. Aziz, M. Waseem, S. Liu, Y. Ma, Z. Lin, and Q.-U.-D. Memon, "A self-healing restoration of power grid based on two-stage adaptive decision-making strategy to enhance grid resilience," *International Journal of Electrical Power & Energy Systems*, vol. 154, p. 109435, 2023.

[12] A. Golshani, W. Sun, Q. Zhou, Q. P. Zheng, and J. Tong, "Two-stage adaptive restoration decision support system for a self-healing power grid," *IEEE Transactions on Industrial Informatics*, vol. 13, no. 6, pp. 2802–2812, 2017.

[13] M. Alhazmi and P. Li, "Advancing resilient power systems through hierarchical restoration with renewable resources," *Scientific Reports*, vol. 15, p. 29755, 2025.

[14] P. Lyu, Q. Bu, Y. Liu, J. Jing, J. Hu, L. Su, and Y. Chu, "Power restoration optimization strategy for active distribution networks using improved genetic algorithm," *Biomimetics*, vol. 10, no. 9, 2025.

[15] A. Rahman, W. Sun, and H. Haggi, "Cyber threat susceptibility assessment of hydrogen infrastructure," in *Proceedings of the 2025 IEEE Power and Energy Society General Meeting (PESGM)*. Austin, Texas, USA: IEEE, 2025, pp. 1–5.

979-8-3315-8138-1